Research Article
doi: 10.1590/01047760202330013367
vol(30), 2024

CERNE

Apparent density of eucalyptus wood evaluated by digital X-ray images after storage in the field during 365 days

Raiana Augusta Grandal Savino Barbosa[1], Vinícius Resende de Castro[1], Paula Gabriella Surdi[1], William Moreira de Oliveira[1], Caio Cesar Nemer Martins[1*], Antônio José Vinha Zanuncio[2], José Cola Zanuncio[1], Angélica de Cássia Oliveira Carneiro[1], Solange de Oliveira Araújo[3]

[1]Federal University of Viçosa, Viçosa, MG, Brazil
[2]Federal University of Uberlândia, Monte Carmelo, MG, Brazil
[3]University of Lisbon, Lisbon, Portugal

TECHNOLOGY OF FOREST PRODUCTS

ABSTRACT

Background: The use of X-rays non-destructive technique in color scale in 2D and 3D needs further studies to understand variations in the apparent density of wood stored under natural conditions. The objective of this study was to evaluate, by digital X-ray images and to test the rainbow scale in digital X-ray images in 2D and 3D, the apparent density of eucalyptus wood after storage in the field during 365 days. Trees of two diametric classes were randomly distributed at three heights in a pile in direct contact with the soil. The apparent density of the wood and its diametric profiles in the radial direction were determined using digital X-ray images in gray scale, and converted to a rainbow scale and the density variations plotted on a 3D surface.

Results: The wood density decreased as the storage period increased. The density of the samples at 0 days of storage evaluated with the 3D images was homogeneous, while an intense attack by xylophagous organisms due to the exposure to the environmental conditions was observed in those collected at 365 days of storage.

Conclusion: The rainbow scale color from X-ray images facilitated to visualize and to interpret the variation of apparent density distribution of the wood.

Keywords: Forest biomass; Storage, X-ray densitometry.

HIGHLIGHTS

The apparent density of *Eucalyptus* wood, assessed by X-ray densitometry, decreased as the storage period increased.
The greatest drop in density occurred in the smaller diameter logs located at the bottom of the pile.
The greater color variability of the rainbow scale facilitated to visualize and to interpret the variation in the apparent wood density.
Fungal attack during the period of air drying increased the variability of wood density within the same sample.

BARBOSA, R. A. G. S.; CASTRO, V. R.; SURDI, P. G.; OLIVEIRA, W. M.; MARTINS, C. C. N.; ZANUNCIO, A. J. V.; CARNEIRO, A. C. O. Apparent density of eucalyptus wood evaluated by digital x-ray images after storage in the field during 365 days. CERNE, v.30, e-103367, doi: 10.1590/01047760202430013367.

✤Corresponding author: caio.martins@ufv.br
Received: December 12/2023 Accepted: May 16/2024

Open Access
CERNE
ISSN 0104-7760
UNIVERSIDADE FEDERAL DE LAVRAS

INTRODUCTION

Brazil has 9.94 million hectares of planted forests, with 7.6 million hectares belonging to the genus *Eucalyptus*, with an average productivity of 32.7 m³/ha/year (Ibá, 2023). This wood is used for energy generation and pulp production, in both cases, the wood needs to be stored in the field (Zanuncio et al., 2017; Silva et al., 2023).Post-harvest log management requires planning, especially in storage, part of the pre-treatment of biomass to reduce transportation costs and improve its conversion into energy (Zanuncio et al., 2017; Giesel et al., 2020).

The average wood storage time practiced by forestry companies of 60 days does not result in significant losses in wood density. However, the storage period must be sufficient to reduce the moisture content without loss of dry wood mass, which can result in an increase in storage time (Kuptz et al., 2020). In this way, wood that requires longer storage periods can undergo changes that reduce its quality and increase energy losses due to factors such as biodeterioration by xylophagous organisms and weathering, for example, which can result in a loss of density (Medeiros et al., 2020; Nandika et al., 2020).

Density is one of the most important indices in the evaluation of the wood quality and it is easy to determine and correlates with other properties, such as dimensional stability (Pelit et al., 2018), water flow (Zanuncio et al., 2022), carbon fixation (Gao et al., 2018), and climate change (Gao et al., 2018). The use of more precise methods such as X-ray densitometry to determine this parameter has increased because they are non-destructive, fast, dispensing reagents and solvents and allowing to precisely obtaining the apparent density of the wood radial profile (Jacquin et al., 2017). Variations in the growth of trees with different fertilization and silvicultural practices, in addition to carbon fixation were also evaluated with 2D digital X-ray images (Mannes et al., 2007; Keunecke et al., 2012; Cherubini et al., 2013; Castro et al., 2020).

Therefore, based on the hypothesis that X-ray densitometry technique is capable of determining wood density quickly, accurately, and non-destructively, the objective of this study was to assess, through digital images, the apparent density of wood after field storage for 365 days, and to test the use of rainbow scale in 2D and 3D X-ray digital images for evaluating this parameter of a hybrid of *Eucalyptus urophylla* × *Eucalyptus grandis*.

MATERIAL AND METHODS

Source of the material

Trees of the commercial clone AEC 1528 (*Eucalyptus urophylla* × *Eucalyptus grandis* hybrid), seven years old, were selected with a minimum diameter at breast height (DBH) of 6 cm and harvested in a plantation in the municipality of Viçosa, Minas Gerais, Brazil (20º 47 ‘56, 80” S and 42º 49 ‘58.60” O).

Data acquisition

The wood biomass quality was evaluated at different storage periods with one-meter long logs with bark and stacked outdoors. These logs were divided into two diametric classes (DC) of DCI (DBH ≤ 11 cm and minimum of 6 cm) and DCII (DBH ≥ 11.1 cm, with a maximum of 14 cm), and randomly distributed at three heights (upper, intermediate and lower) in a seven-meter-long pile (Figure 1) in direct contact with the ground and oriented in the East-West direction to maximize exposure to solar radiation.

Three logs per diametric class were randomly selected at harvest to obtain data at time 0 (zero day of log collection). X-ray every 60 days, except the last one at 120 days after the previous one, totaling 365 days of evaluation from October 10, 2018 to October 10, 2019. The selection of logs, for sampling, disregarded those along a meter on each side of the pile, to avoid possible border effects. Climate data from the Automatic Station of Viçosa (MG), located at the Federal University of Viçosa (UFV) (20° 45’ 45.385” S and 42° 51’ 50.447” W), were collected during the experiment period (Figure 2).

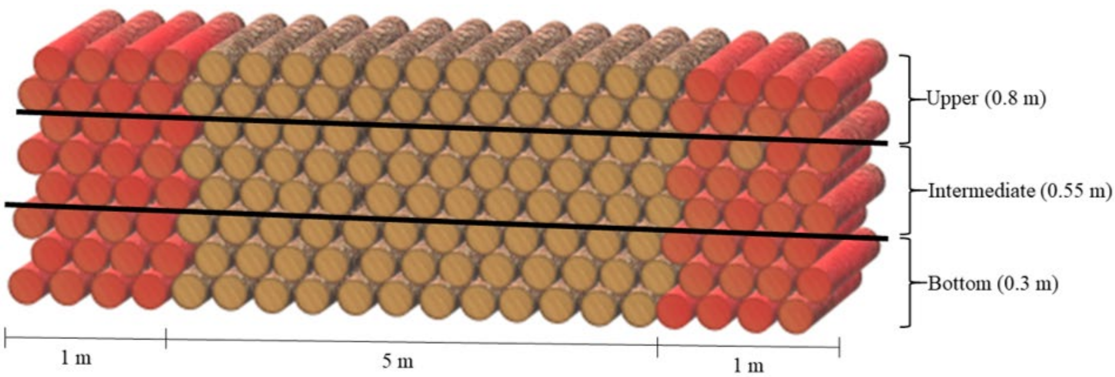

Figure 1: Scheme with the dimensions of the pile of eucalyptus wood logs with those marked with red disregarded in the sampling.

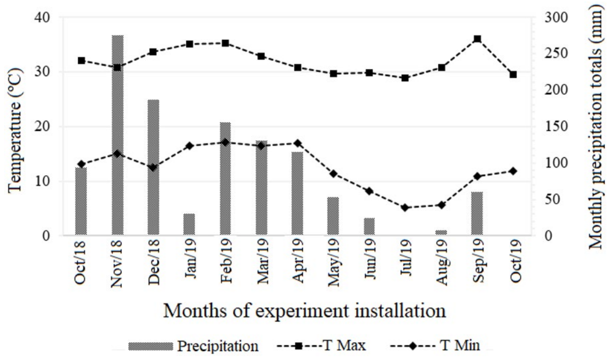

Figure 2: Precipitation and maximum and minimum temperature data during the execution period of the experiment.

Five logs, by diametric class and height/position in the pile (upper, intermediate and bottom), were removed every 60 days to evaluate their wood properties. The logs collected in the upper and bottom positions were those in full sun and in direct contact with the ground, respectively. Each log was divided into four equidistant positions along the longitudinal axis, with positions A and D corresponding to the ends, and B and C to the central positions, from which three disks with a thickness of about 4 cm were removed for analysis (Figure 3).

The discs were cut into diametric sections, from which 2 mm thick samples were taken radially, and placed in a climatized environment (20 ºC and 60% relative humidity) to determine the apparent density of the wood by X-ray digital images (Gaitan-Alvarez et al., 2019; Castro et al., 2020). There is a relationship between x-ray reflectance and wood density, allowing the use of x-ray images as a non-destructive method of wood evaluation. Wood density varies in the pith-bark direction, being lower in the central region, to capture this heterogeneity, it is necessary cross the center of the disc in the evaluation in the X-ray digital images evaluation.

Thus, the apparent density and the diametric profiles was evaluated in the radial direction of the wood, were determined in these digital images, in gray scale and in those generated by the X-ray equipment (Faxitron model LX 60 – 26 Kv and exposure time of 19 seconds) and ImageJ software and the data transferred to spreadsheet (Castro et al., 2020; Curvo et al., 2024). The gray images were converted to a rainbow scale with Adobe Photoshop software and the density variations plotted on a 3D surface with the aid of the ImageJ software. The surface of the wood was plotted in 3D with narrow lines, parallel to each other and perpendicular to the length of the samples to better visualize the variation of the apparent density of the wood throughout the sampling period.

The experiment was in a factorial scheme (6 x 3 x 2) with the collection time (0, 60, 120, 180, 240 and 365 days), position of the log in the pile (upper, intermediate and bottom) and diametric class (6-11 cm and 11-14 cm) with 36 treatments and three replications. The data were submitted to the normality test (Shapiro-Wilk) and their non-normality found. For this reason, the medians were compared using the Kruskal-Wallis test at 5% significance with the Action Stat software, version 3.7.

RESULTS AND DISCUSSION

The medians of the apparent density of the wood, obtained by X-ray densitometry at the beginning of the experiment (day zero), ranged from 0.513 to 0.500 g.cm^{-3} (Figure 4) the diameter of the logs did not influence the density values. The apparent density values of the *E. urophylla* × *E. grandis* hybrid logs were similar to those found in other studies, 0.420 to 0.600 g.cm^{-3} for species of the genus Eucalyptus (Tomazello et al., 2008; Knapic et al., 2014; Chambi-Legoas et al., 2023).

*The uppercase letters analyzed the differences between days, and the lowercase letters analyzed the differences between the diameter classes (DC) of the logs associated with their positions in the pile, each storage period. Values followed by the same letter (upper or lower case) per bar do not differ from each other using the Kruskal-Wallis test at 5% probability.

The apparent density of the wood decreased as the storage period increase with a reduction of 11.3% and 6.2%, 16.2% and 8.8% and 16.2% and 4.6%, at the end of the 365 days, for the logs of smaller and larger diametric classes, removed from the upper, intermediate and bottom regions of the pile, respectively (Figure 4). The apparent density medians of the eucalyptus samples, with smaller and larger diameter classes, obtained with the X-ray densitometry method after 12 months of storage, were 0.455, 0.430 and

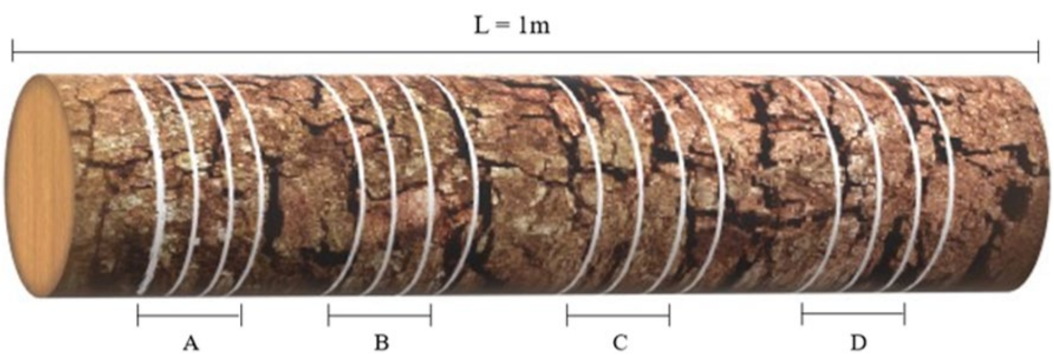

Figure 3: Sectioning position to removing the discs in the longitudinal direction of the logs to assess their density.

0.430 g.cm^{-3} and 0.469, 0.456 and 0.477 g.cm^{-3} in the upper, middle and bottom regions of the storage pile, respectively (Figure 5). At the end of storage period (365 days), the bulk density of samples of smaller and larger diameter classes decreased in the radial direction.

The decrease in the apparent density over the storage period is associated with variations in this parameter in the radial direction due to the deterioration of wood after 60 days of exposure in the field to xylophagous organisms, such as decaying fungi and termites in high humidity conditions, accelerating the deterioration process (Santini Jr et al., 2019). The losses in the apparent density of the wood in the lower position for the smallest diameter class and in the intermediate one for the largest class can be explained by the fact that the wood exposed to the environment, leads to the cellulose depolymerization and losses of hemicellulose content and lignin. This is due to oxygen and moisture in ideal values for the deterioration and the effect of ultraviolet light inducing photochemical reactions in the wood. The storage period must be sufficient to reduce the moisture content in the biomass without losing characteristics influencing other properties (Avila et al., 2016; Chang et al., 2020).

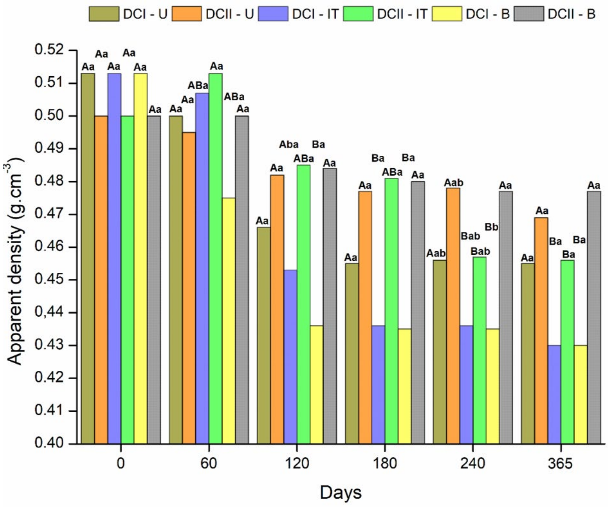

*The uppercase letters analyzed the differences between days, and the lowercase letters analyzed the differences between the diameter classes (DC) of the logs associated with their positions in the pile, each storage period. Values followed by the same letter (upper or lower case) per bar do not differ from each other using the Kruskal-Wallis test at 5% probability.

Figure 4: Apparent density of wood (g.cm^{-3}) by X-ray densitometry of eucalyptus logs by diameter class, where DCI = DAP ≤ 11 cm and a minimum of 6 cm and DCII = DAP ≥ 11.1 cm, with a maximum of 14 cm), position in the pile (U = Upper, IT = intermediate and B = Lower) and storage period (0, 60, 120, 180, 240 and 365 days).

The attack by fungi of the white and soft rot in the woods of smaller diameters was in the radial direction (Figure 5) and in the sapwood and heartwood in those of larger diameters. White and black spots (Figures 5a, 5b, 5c and 5d), visible to the naked eye in the woods of the two diametric classes were more accentuated in those in the lower region of the pile with direct contact with the soil. The presence of dark lines in the wood throughout the storage period, besides particulate material released from the larger diameter logs when rubbed was observed. This is associated to damage by fungi of white and soft rot, in the smaller diameter woods in the radial direction and in the sapwood and heart-peripheral regions in those of larger diameter.

These xylophagous organisms degraded the cell wall constituents, lignin and carbohydrates, reducing the wood density, as reported for those of *Eucalyptus grandis × Eucalyptus urophylla*, *Tipuana tipu* and *Fagus sylvatica* (Hervé et al., 2014; Santini Jr et al., 2019; Cantera et al., 2022). This makes the wood more permeable and hygroscopic, affecting its anatomical and mechanical properties and leaving it more susceptible to rupture by simple traction (Brazolin et al., 2014; Dahali et al., 2021). The dark (black) lines in the wood are called zone lines, composed of melanin, characteristics of spalted wood and are formed by two or more white rot fungi species (Morris et al., 2021).

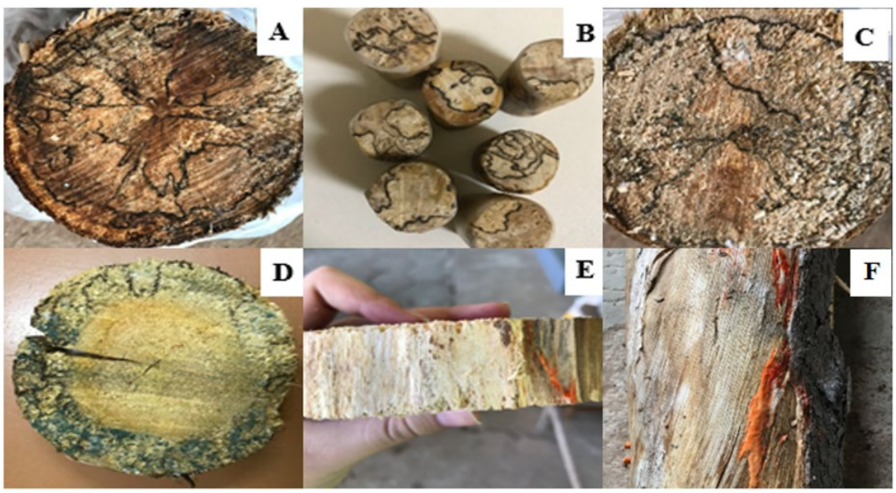

Figure 5: *Eucalyptus* woods at 365 days of storage with signs of white (5a, 5b, 5c and 5d) and soft (5d), spalted wood (5a, 5b, 5c and 5d), and apparent defibrillation (5e and 5f).

Trametes versicolor, mainly, develops such zone lines when detecting in the wood the presence of another fungus of equivalent strength (Bari et al., 2019). Soft rot fungi develop in conditions of high humidity and deteriorate the wood more slowly than the white and brown ones (Karunasekera et al., 2017), the latter extensively deteriorate polysaccharides and leaving regions with lignin residues (Singh, 2012).

The apparent density values in the wood pith region, of the two diameter classes, at the beginning of the experiment (day zero) were high, followed by a decrease and an increase trend in the pith-bark direction. In addition, characteristic signs of growth bands, such as distinct fibrous zones indicated in the gray scale by lighter regions (high density) and in the rainbow (colored) by reddish tones were observed (Figure 6).

The higher apparent density in the region near the wood pith of the two diametric classes is associated to the presence of reserve substances (starch crystals) in the cells of their axial parenchyma (Castro et al., 2020). The increase in the apparent density in the pith-bark direction agrees with what reported for juvenile woods of *Eucalyptus* sp. (Arantes et al., 2016; Castro et al., 2017; Castro et al., 2020) and it is associated to variations caused by alternations in diameter and frequency of vessel elements and fiber strips with thicker walls. Growth bands, such as fibrous zones indicated in the gray-scale X-ray images for the lighter regions and in the rainbow (colored) scale for the red ones, indicate greater X-ray attenuation and, therefore, higher apparent density (Castro et al., 2017).

The color palette of the rainbow scale facilitates the interpretation and identification of regions with different densities along the radial wood profile, ranging from blue (lower density) to red (higher density) (Medeiros et al., 2020). The differentiation of wood density by colors on the rainbow scale allowed a greater contrast than that of the gray one, indicating that this methodology is appropriate to determining this parameter. Lighter regions (gray scale) or reddish tones (rainbow scale) indicate layers of fibers with a thick cell wall and small number of vessels with smaller diameters (Zanuncio et al., 2018). This makes possible to

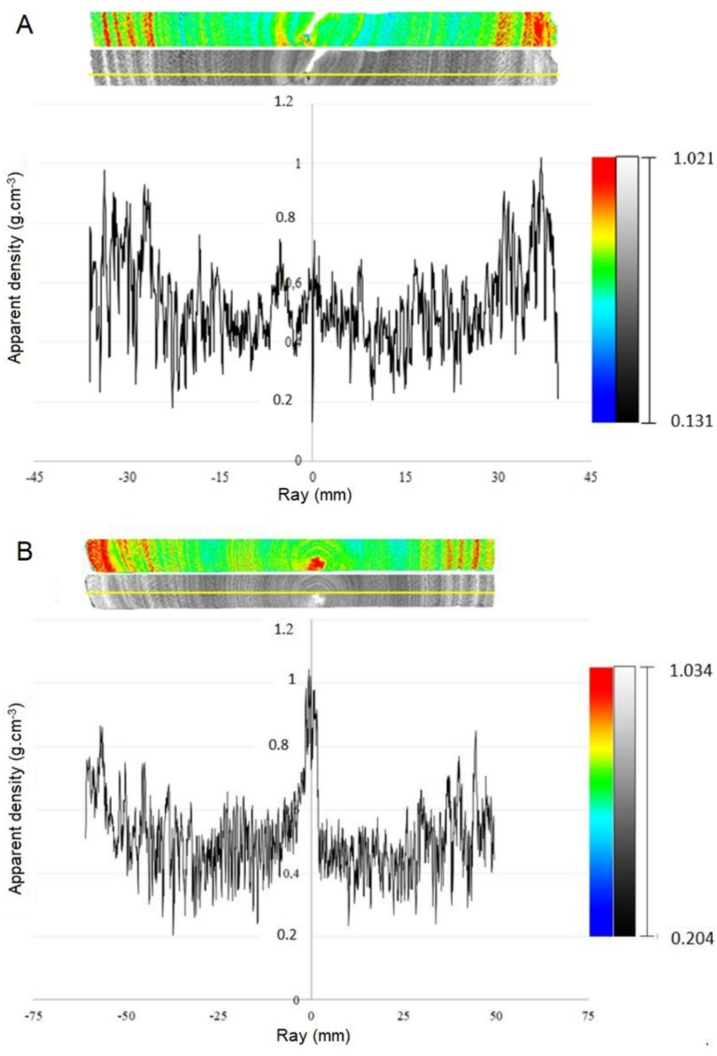

Figure 6: Profile of the apparent density of *Eucalyptus* samples with lower (a) and higher (b) diametric class on day 0 of storage.

demarcate and measure, by X-ray irradiation, the width of the growth rings from digital images of the wood of the trees (Castro et al., 2017). The results of the methodology using X-ray images with different shades were also satisfactory in the evaluation of quality, physiology and internal seed morphology (Trujillo et al., 2019; Medeiros et al., 2020).

The density variation, in the densitometric profiles of the samples in the two diameter classes at different heights and at 365 days of storage (Figure 7), was smaller in the logs of the upper position with lower blue and dark tones (black) in the images of the scale rainbow and gray, respectively. The density variability, in the samples of the bottom position, was greater with more accentuated alternation between peaks and valleys, in addition to the greater presence of the shades of blue and black in the images of the rainbow and gray scale, respectively, in the heartwood and sapwood. The apparent density in the pith-shell direction tended to increase in the samples of the upper and intermediate position in the two diametric classes.

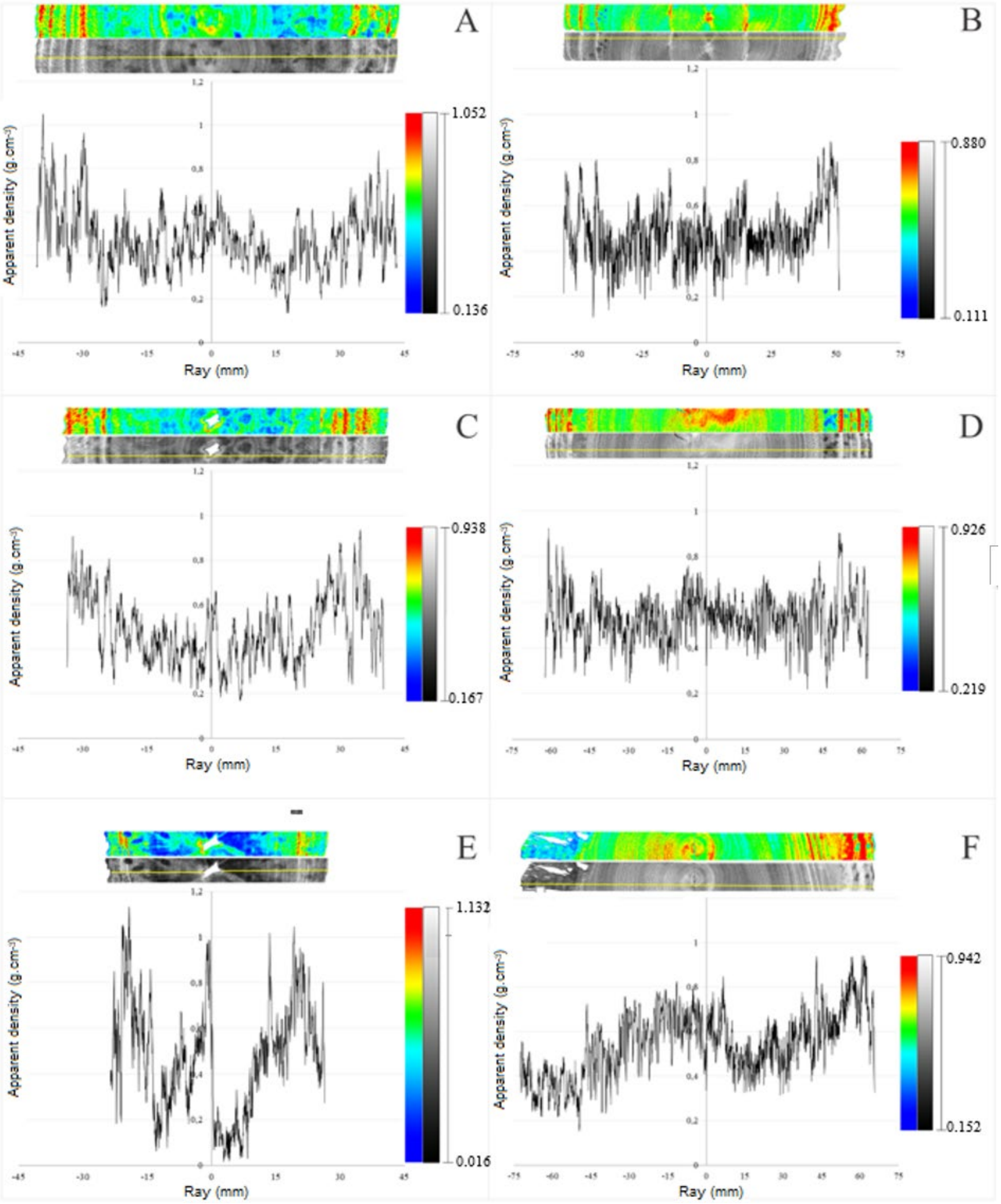

Figure 7: Profile of the apparent density at 365 days of storage in the wood of *Eucalyptus* samples with a lower diameter class in the upper (7a), intermediate (7c) and bottom (7e) regions, respectively, and a higher diameter class in the upper (7b), intermediate (7d) and bottom (7f) regions, respectively.

The lower apparent density in the samples from the lower position in the two diameter classes after 365 days of storage may be due to the attack by fungi. This increases the permeability and, consequently, the hygroscopic capacity of the wood due to the anatomical and chemical changes of the cell wall components, with destruction of the membranes and reduction of the mechanical properties in the wood and, consequently, defibrillation (Pinheiro et al., 2020). The better conditions for deterioration by bacteria, fungi and insects, responsible for part of the wood mass reduction, explains the presence of holes and the reduction in the thickness of the secondary cell wall, besides the deterioration of the parenchyma and middle lamella in the advanced stages of attack by xylophagous organisms as in the samples from the lower position at 365 days of storage (Bari et al., 2019). In addition, the amount of sapwood in the smaller diameter woods is higher and, consequently, more permeable. This leaves this region more vulnerable to colonization by fungi with a significant loss of wood mass in the medium/long term (Leonhardt et al., 2019), and consequently decreasing the apparent density of the wood.

The direct contact of the wood with the soil is another factor that may have contributed to the lower apparent density in the samples from the bottom position. The soil loses moisture more slowly than the wood and the microbiota in the wood is richer in decomposing microorganisms that may have acted more in the material in contact with the soil, thus accelerating the density reduction. Furthermore, the decrease in the apparent density due to the deterioration of wood by xylophagous organisms becomes more significant under conditions of direct contact with water through precipitation or direct contact with the soil (Brischke and Alfredsen, 2020).

The apparent density of the wood from the plot of its surface in 3D was heterogeneous throughout the sample (Figure 8). The number of peaks and valleys in the same line is directly related to variations in the wood density in the region sampled. The distribution of peaks and valleys throughout the wood, in the samples of the control wood in the first day of storage, was greater in the 3D images. The apparent wood density at 0 days of storage was more homogeneous along the samples than in those collected at 365, the latter with intense attack by xylophagous organisms and exposure to environmental conditions. The 3D plotting of the density surface by colors and lines on the rainbow scale was better than with gray scale to assess the apparent density of eucalyptus wood.

The heterogeneity of the apparent wood density, from the plot of its surface in 3D, influence its technological properties, with the deterioration of the cell wall and consequent reduction of this parameter throughout the storage period (Ringman et al., 2019). The increase in the distribution of peaks and valleys in the same line throughout the sample indicates greater variability in the wood density along its length, which may cause problems for its use due to the effect of this parameter on some of its other properties, such as anatomy, chemistry and mechanics. The color variation, with blue and red lines, indicates lower and higher density, respectively, and that the 3D plot of the surface improved the visualization and interpretation of the apparent wood density variation over the sample using digital X-ray images. The greater homogeneity of the peak valley distribution along the entire wood in the images with plotting the surface in 3D of the wood samples in the control (first day of storage) than in those at 365 days, especially in samples in the lower region of the pile storage, is due to the greater exposure of wood to xylophagous organisms (Nurmi, 1995).

The three-dimensional structure of the internal region of the materials studied and the increased speed of data analysis confirm satisfactory results, with the use of the 3D scale to study the density of the wood and its growth rings (Van der Bulcke et al., 2014), and the seed integrity (Medeiros et al., 2020). The use of X-ray images, in gray scale or with color gradient in 2D and 3D, are non-destructive and important methods as an additional methodology to the traditional laboratory technological characterization (Rousseau et al., 2015; Abud et al., 2018). The proposed method provides a quick, easy to interpret and reliable solution to assess the apparent density, by X-rays, of *Eucalyptus* wood from digital images.

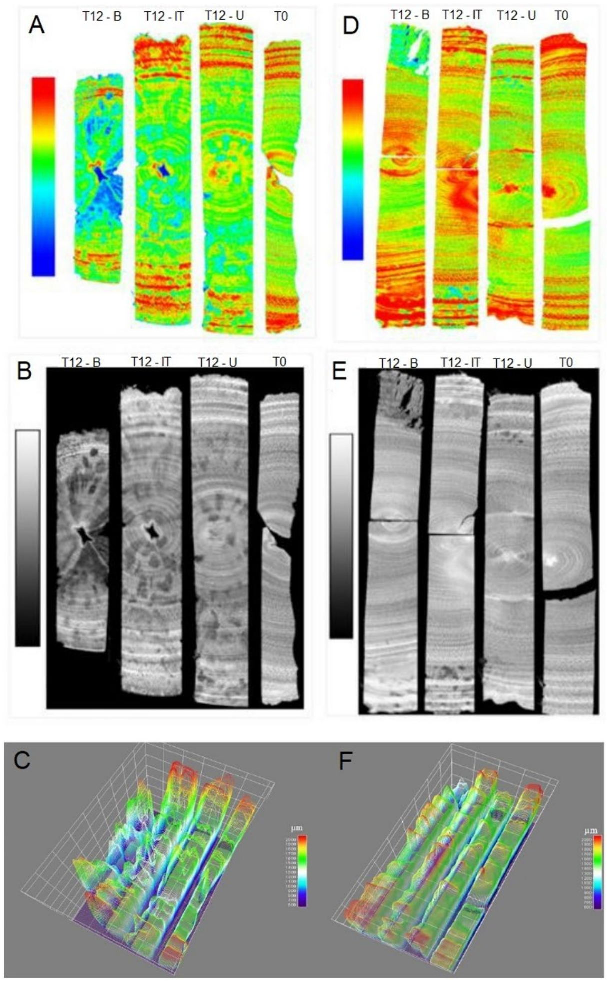

Figure 8: Samples at 0 (T0) and 365 (T12) days of storage of wood with smaller (DCI) and larger (DCII) diameter classes with the rainbow (8a and 8d) and gray (8b and 8e) scale and plotting the 3D density variation surface (8c and 8f).

CONCLUSIONS

The apparent density of eucalyptus wood, assessed by X-ray densitometry, decreased as the storage period increased. After 60 days of exposure, there may be a significant loss of density along the radial direction, with the position in the pile, the diameter of the log and climatic conditions influencing the speed of wood deterioration. The decrease in the apparent density over the storage period is associated with variations in this parameter in the radial direction due to the deterioration of wood after 60 days of exposure in the field to xylophagous organisms, such as decaying fungi and termites in high humidity conditions, accelerating the deterioration process The greatest drop in density occurred in the smaller diameter logs located at the bottom of the pile due the direct contact with the ground. The greater color variability of the rainbow scale facilitated to visualize and to interpret the variation in the apparent wood density. This methodology, associated with the plotting of the wood surface in 3D, improved the visualization of the apparent density variation of this material by the arrangement of lines in 3D scale. Fungal attack during the period of air-drying increased the variability of wood density within the same sample. In this way, the X-ray densitometry technique used in monitoring the density of wood stored for 365 days allowed for the identification of the minimum storage time for significant loss of wood density. This information can be useful for companies that need to store wood for a longer period than usual.

AUTHORSHIP CONTRIBUTION

Project Idea: RAGSB, VRC, PGS, ACOC

Database: RAGSB, VRC

Processing: RAGSB, VRC, WMO, CCNM

Analysis: RAGSB, VRC, PGS

Writing: RAGSB, AJVZ, JCZ, CCNM, SOA

Review: VRC, AJVZ, JCZ, CCNM, ACOC, SOA

ACKNOWLEDGMENTS

Funding: This work was supported by the Brazilian agencies Conselho Nacional de Desenvolvimento Científico e Tecnológico (CNPq), Fundação de Amparo à Pesquisa de Minas Gerais (FAPEMIG), Coordenação de Aperfeiçoamento de Pessoal de Nível Superior (CAPES) and support from Solange de Oliveira Araújo through a research contract through FCT (DL57/2016/CPI382/CT0018) and Fundação para a Ciência e a Tecnologia, I.P., by project reference UIDB/00239/2020 from the Forestry Research Center, DOI 10.54499/UIDB/00239/2020.

REFERENCES

ABUD, H. F.; CICERO, S. M.; JUNIOR, F. G. G. Radiographic images and relationship of the internal morphology and physiological potential of broccoli seeds. Acta Scientiarum. Agronomy, v. 40, p. e34950, 2018.

ARANTES, M. D. C.; TRUGILHO, P. F.; TOMAZELLO FILHO, M.; et al. DENSITOMETRIA DE RAIOS X NA MADEIRA E CARVÃO DE CLONE DE *Eucalyptus grandis* W. Hill ex Maiden X *Eucalyptus urophylla* ST Blake. Revista Árvore, v. 40, n.1, p. 155-162, 2016.

DELUCIS, R. A.; CADEMARTORI, P. H. G.; MISSIO, A. L.; et al. Decay resistance of four fast-growing eucalypts wood exposed to three types of fields. Maderas. Ciencia y tecnología, v. 18, n. 1, p. 33-42, 2016.

BARI, E.; DARYAEI, M. G.; KARIM, M.; et al. Decay of *Carpinus betulus* wood by *Trametes versicolor* - An anatomical and chemical study. International Biodeterioration & Biodegradation, v. 137, p. 68-77, 2019.

BRAZOLIN, S.; FILHO, M. T.; YOJO, T.; et al. Propriedades físico-mecânicas do lenho deteriorado por fungos apodrecedores de árvores de Tipuana tipu. Cerne, v. 20, v. 2, p. 183-190, 2014.

BRISCHKE, C.; ALFREDSEN, G. Wood-water relationships and their role for wood susceptibility to fungal decay. Applied microbiology and biotechnology, v. 104, n.9, p. 3781-3795, 2020.

CANTERA, L.; ALONSO, R.; LUPO, S.; et al. Decay resistance of thermally modified *Eucalyptus grandis* wood against wild strains of *Trametes versicolor* and *Pycnoporus sanguineus*. Wood Material Science & Engineering, v. 17, n. 6, p. 478-487, 2022.

CASTRO, V. R.; SURDI, P. G.; SETTE, C. R.; et al. Efeito da aplicação do potássio, do sódio e da disponibilidade hídrica na densidade aparente a 12% de umidade do lenho juvenil de árvores de *Eucalyptus grandis*. Ciência Florestal, v. 27, n.3, p. 1017-1027, 2017.

CASTRO, V. R.; CHAMBI-LEGOAS, R.; FILHO, M. T.; et al. RETRACTED ARTICLE: The effect of soil nutrients and moisture during ontogeny on apparent wood density of *Eucalyptus grandis*. Scientific reports, v. 10, n. 1, p. 2530, 2020.

CHAMBI-LEGOAS, R.; TOMAZELLO-FILHO, M.; LACLAU, J. P.; et al. Potassium fertilization enhances xylem plasticity and growth recovery of *Eucalyptus grandis* trees in response to drastic changes in water availability. Forest Ecology and Management, v. 528, p. 120656, 2023.

CHANG, L.; RONG, B.; XU, G.; et al. Mechanical properties, components and decay resistance of *Populus davidiana* bioincised by *Coriolus versicolor*. Journal of Forestry Research, v. 31, n. 5, p. 2023-2029, 2020.

CHERUBINI, P.; HUMBEL, T.; BEECKMAN, H.; et al. Olive tree-ring problematic dating: a comparative analysis on Santorini (Greece). PloS one, v. 8, n. 8, p. e54730, 2013.

CURVO, K. R.; SILVA, G. A. O.; CASTRO, V. R., et al. Heartwood proportion and density of *Tectona grandis* Lf wood from Brazilian fast-growing plantations at different ages. European Journal of Wood and Wood Products, v. 82, p. 357–369, 2024.

DAHALI, R.; MD. TAHIR, P.; ROSELEY, A. S. M.; et al. Influence of *Chrysoporthe deuterocubensis* canker disease on the physical and mechanical properties of *Eucalyptus urograndis*. Forests, v. 12, n. 5, p. 639, 2021.

GAITAN-ALVAREZ, J.; MOYA, R.; BERROCAL, A. The use of X-ray densitometry to evaluate the wood density profile of *Tectona grandis* trees growing in fast-growth plantations. Dendrochronologia, v. 55, p. 71-79, 2019.

GAO, B.; TAYLOR, A. R.; SEARLE, E. B.; et al. Carbon storage declines in old boreal forests irrespective of succession pathway. Ecosystems, v. 21, p. 1168-1182, 2018.

GIESEL, G.; BRAND, M. A.; MILAGRES, F. R.; et al. Effect of the log storage of *Pinus taeda* L. on the quality of kraft pulp. Floresta, v. 50, n. 4, p. 1844-1853, 2020.

JACQUIN, P.; LONGUETAUD, F.; LEBAN, J. M.; et al. X-ray microdensitometry of wood: A review of existing principles and devices. Dendrochronologia, v. 42, p. 42-50, 2017.

INDÚSTRIA BRASILEIRA DE ÁRVORES. Relatório Ibá 2023. São Paulo, 2023. 91 p.

HERVÉ, V.; MOTHE, F.; FREYBURGER, C.; et al. Density mapping of decaying wood using X-ray computed tomography. International Biodeterioration & Biodegradation, v. 86, p. 358-363, 2014.

KNAPIC, S.; PIRRALHO, M.; LOUZADA, J. L.; et al. Early assessment of density features for 19 *Eucalyptus* species using X-ray microdensitometry in a perspective of potential biomass production. Wood Science and Technology, v. 48, p. 37-49, 2014.

KARUNASEKERA, H.; TERZIEV, N.; DANIEL, G. Does copper tolerance provide a competitive advantage for degrading copper treated wood by soft rot fungi?. International Biodeterioration & Biodegradation, v. 117, p. 105-114, 2017.

KEUNECKE, D.; NOVOSSELETZ, K.; LANVERMANN, C.; et al. Kombination von Röntgenmessung und digitaler Bildkorrelation zur Dehnungsanalyse an Holz: Potential und Schwierigkeiten. European Journal of Wood and Wood Products, v. 70, p. 407-413, 2012.

KUPTZ, D.; LECHE, S.; MENDEL, T.; et al. Fuel properties, dry matter losses, and combustion behavior of wood chips stored at aerobic and anaerobic conditions. Biomass and Bioenergy, v. 142, p. 105745, 2020.

LEONHARDT, S.; HOPPE, B.; STENGEL, E.; et al. Molecular fungal community and its decomposition activity in sapwood and heartwood of 13 temperate. European tree species. PloS one, v. 14, n. 2, p. e0212120, 2019.

MANNES, D.; LEHMANN, E.; CHERUBINI, P.; et al. Neutron imaging versus standard X-ray densitometry as a method to measure tree-ring wood density. Trees, v. 21, p. 605-612, 2007.

MEDEIROS, A. D.; SILVA, L. J.; PEREIRA, M. D.; et al. High-throughput phenotyping of brachiaria grass seeds using free access tool for analyzing X-ray images. Anais da Academia Brasileira de Ciências, v. 92, n. suppl 1, p. e20190209, 2020.

NETO, P. N. M.; PAES, J. B.; OLIVEIRA, J. T. D. S.; et al. Durability of *Eucalyptus* wood in soil bed and field decay tests. Maderas. Ciencia y tecnología, v. 22, n. 4, p. 447-456, 2020.

MORRIS, H.; SMITH, K. T.; ROBINSON, S. C.; et al. The dark side of fungal competition and resource capture in wood: Zone line spalting from science to application. Materials & Design, v. 201, p. 109480, 2021.

NANDIKA, D.; DARMAWAN, W.; KARLINASARI, L.; et al. Evaluation of color change and biodeterioration resistance of Gewang (*Corypha utan* Lamk.) wood. Applied Sciences, v. 10, n. 21, p. 7501, 2020.

NURMI, J. The effect of whole-tree storage on the fuelwood properties of short-rotation Salix crops. Biomass and Bioenergy, v. 8, n. 4, p. 245-249, 1995.

PELIT, H.; BUDAKÇI, M.; SÖNMEZ, A. Density and some mechanical properties of densified and heat post-treated Uludağ fir, linden, and black poplar woods. European Journal of Wood and Wood Products, v. 76, p. 79-87, 2018.

PINHEIRO, C. G.; BIANCHINI, N. H.; PAVLACK, A. S.; et al. A METHOD FOR EVALUATING ERGOSTEROL CONTENT IN WOOD-DECAY FUNGI. Revista Árvore, v. 44, p. e4410, 2020.

RINGMAN, R.; BECK, G.; PILGÅRD, A. The importance of moisture for brown rot degradation of modified wood: a critical discussion. Forests, v. 10, n. 6, p. 522, 2019.

ROUSSEAU, D.; WIDIEZ, T.; TOMMASO, S. D.; et al. Fast virtual histology using X-ray in-line phase tomography: application to the 3D anatomy of maize developing seeds. Plant Methods, v. 11, n.55, p. 1-10, 2015.

SANTINI JR, L.; RODRIGUEZ, D. R. O.; QUINTILHAN, M. T.; et al. Evidence of wood biodeterioration of tropical species revealed by non-destructive techniques. Science of the Total Environment, v. 672, p. 357-369, 2019.

SILVA, W. M.; ZANUNCIO, A. J. V.; CARVALHO, A. G.; et al. Drying of eucalyptus logs from plantations with different spacing between trees. Bioresources, v. 18, n. 1, p. 1177-1184, 2023.

SINGH, A. P. A review of microbial decay types found in wooden objects of cultural heritage recovered from buried and waterlogged environments. Journal of Cultural Heritage, v. 13, n. 3, p. 16-20, 2012.

TOMAZELLO, M.; BRAZOLIN, S.; CHAGAS, M. P.; et al. Application of X-ray technique in nondestructive evaluation of eucalypt wood. Maderas. Ciencia y tecnología, v. 10, n. 2, p. 139-149, 2008.

TRUJILLO, H. A.; GUILHIEN GOMES-JUNIOR, F.; LARA, I. A. R. D.; et al. Radiographic analysis and performance of coffee seeds. Journal of Seed Science, v. 41, n.4, p. 431-440, 2019.

BULCKE, J. V. D.; WERNERSSON, E. L. G.; DIERICK, M.; et al. 3D tree-ring analysis using helical X-ray tomography. Dendrochronologia, v. 32, n. 1, p. 39-46, 2014.

ZANUNCIO, A. J. V.; CARVALHO, A. G.; SILVA, M. G. D.; et al. Importance of wood drying to the forest transport and pulp mill supply. Cerne, v. 23, n.2, p. 147-152, 2017.

ZANUNCIO, A. J. V.; CARVALHO, A. G.; CARNEIRO, A. D. C. O.; et al. Anatomical, ultrastructural, physical and mechanical wood properties of two-year-old *Eucalyptus grandis* x *Eucalyptus urophylla* clones. Revista Árvore, v. 42, n.2, p. e420201, 2018.

ZANUNCIO, A. J. V.; da SILVA, W. M.; CARVALHO, A. G.; et al. Basic density in the drying process of *Eucalyptus urophylla* and *Pinus caribaea* wood. Journal of Tropical Forest Science, v. 34, n. 2, p. 142-148, 2022.